Journal of Applied Electrochemistry **32**: 431–438, 2002.

Application of substituted *N*-arylpyrroles in the corrosion protection of aluminium in hydrochloric acid

Z. GRUBAČ[1], R. BABIĆ[2] and M. METIKOŠ-HUKOVIĆ[2]*
[1]*Faculty of Chemical Technology, University of Split, Split, Croatia*
[2]*Department of Electrochemistry, Faculty of Chemical Engineering and Technology, University of Zagreb, Zagreb, Croatia*
*(*author for correspondence, fax: +385 1 4597 139, e-mail: mmetik@marie.fkit.hr)*

Received 1 November 2001; accepted in revised form 19 February 2002

Key words: aluminium, corrosion inhibitors, *N*-arylpyrroles, pickling

Abstract

The inhibiting action of *N*-arylpyrroles on aluminium in 0.17 mol dm^{-3} hydrochloric acid solution, in the temperature range 20–60 °C, was studied using potentiodynamic and electrochemical impedance spectroscopy techniques. The inhibiting efficiency of both investigated compounds 1-(2-fluorophenyl)-2,5-dimethylpyrrole (compound A) and 1-(2-fluorophenyl)-2,5-dimethylpyrrole-3-carbaldehyde (compound B) slightly increases with increasing temperature of the corrosive solution. Inhibitor adsorption on the electrode surface decreases the apparent activation energy of the hydrogen evolution reaction. Compound A follows the Temkin adsorption isotherm, while its carbaldehyde derivative follows the Langmuir isotherm. The results of the apparent energy of activation and the standard free energy of adsorption point to stronger chemisorption of the compound A. However, due to additional condensation of molecules with carbaldehyde groups on the electrode surface, the carbaldehyde derivative exhibits even better inhibiting efficiency than compound A. The kinetic corrosion parameters, analysed in terms of the impedance data, show a satisfactory agreement with those obtained by the potentiodynamic method.

List of symbols

A	Arrhenious preexponential constant (A cm^{-2})
a	molecular interaction parameter
B	Stern–Geary constant (V div^{-1})
b	Tafel slope (V div^{-1})
C	capacitance (F cm^{-2})
c	concentration (mol dm^{-3})
E	potential (V)
E_a	activation energy (J mol^{-1})
f	factor of energetic inhomogeneity of the surface
f	frequency (Hz)
ΔG_{ads}	free energy of adsorption (J mol^{-1})
j	current density (A cm^{-2})
$j\omega$	complex variable for sinusoidal perturbations $\omega = 2\pi f$
K	adsorption constant (dm^3 mol^{-1})
L	inductance (H cm^2)
$\mathscr{R}$	gas constant (8.314 J K^{-1} mol^{-1})
R	resistance (Ω cm^2)
T	absolute temperature (K)
x	number of water molecules replaced by inhibitor molecule
Z	impedance (Ω cm^2)

Greek letters

Θ	phase angle (degree)
θ	surface coverage (%)
η	inhibition efficiency (%)
ω	angular speed (rad s^{-1})
v	sweep rate (V s^{-1})

Sub- and superscripts

o	absence of inhibitor
a.c.	alternating current
ads	adsorption
c	cathodic
corr	corrosion
ct	charge transfer
dl	double layer
el	electrolyte
i	inhibitor
p	polarization

1. Introduction

From the thermodynamic point of view, aluminium is a reactive metal because its standard reduction potential is −1.66 V vs SHE. However, its resistance to corrosion can be attributed to a rapidly formed, thin and highly protective barrier oxide film. This oxide film actively interacts with the solution environment, it grows, transforms, and incorporates solute ions [1]. Among several parameters, solution pH has one of the largest influences on its stability. Below pH 4, the oxide film is less protective due to the active dissolution of the base metal and an increased destabilization of the film [2]. Since HCl solutions are used for pickling of aluminium and its alloys, it is necessary to protect the base metal from the undesirable destructive effect and to improve etching qualities [3]. The practice of inhibition is commonly used to reduce the corrosive attack on metallic materials in acidic solutions. Generally speaking, the action of an inhibitor in aggressive acidic media is assumed to be due to its adsorption at the metal–solution interface [4]. The adsorption process can take place via: (i) electrostatic attraction between the charged metal and the charged inhibitor molecules, (ii) dipole-type interaction between the unshared electron pairs in the inhibitor and the metal, (iii) π-interaction with the metal, and (iv) a combination of all of the above [5]. If the adsorption involves coordinative bonding, the process is termed chemisorption. A number of organic compounds have been described as aluminium corrosion inhibitors in hydrochloric acid solution [6–18], the majority being nitrogen-containing compounds [6, 9–18]. Many *N*-heterocyclic compounds with polar groups and/or π-electrons are efficient corrosion inhibitors in acidic solutions. Organic molecules of this type can absorb on the metal surface and form a bond between the *N* electron pair and/or the π-electron cloud and the metal, thereby reducing corrosion in acidic solution [6, 19].

In a previous study, it was shown that substituted *N*-arylpyrroles act as cathodic-type corrosion inhibitors of aluminium in perchloric [20] and hydrochloric acid solution [21], and of iron in hydrochloric acid solution [22, 23]. It was found that the position and number of functional groups in the pyrrole, or the benzene ring, strongly influence the inhibiting efficiency. The most effective for both metals were 1-(2-fluorophenyl)-2,5-dimethylpyrrole and 1-(2-fluorophenyl)-2,5-dimethylpyrrole-3-carbaldehyde.

The aim of the present work was to study the adsorption characteristics of the above mentioned *N*-arylpyrroles on aluminium in 0.17 mol dm^{-3} hydrochloric acid solution. The influence of temperature on the corrosion and corrosion inhibition of aluminium in the same solution was also studied. The investigation was performed using potentiodynamic and electrochemical impedance spectroscopy (EIS) measurements.

2. Experimental details

The sample selected for the study was 99.6% pure aluminium. The other components were: Fe 0.35, Si 0.09, Zn 0.02 weight percent. Disc electrodes were machined from a cylindrical rod 8 mm in diameter, and moulded in polyester. Prior to each electrochemical experiment, the electrode surface was abraded with emery paper to an 800 metalographic finish, exposed to a hot (40 °C) 1.0 mol dm^{-3} sodium hydroxide solution for 15 s, rinsed with distilled water, left for 10 min in the atmosphere and immersed in the electrolyte solution for 10 min. This procedure gave good reproducibility of results. In all measurements, the counter electrode was a platinum gauze and the reference electrode was a saturated calomel electrode (SCE). All potentials were referred to the SCE.

The measurements were performed in 0.17 mol dm^{-3} hydrochloric acid solution, deaerated with nitrogen, without and with the presence of two substituted *N*-arylpyrroles in the concentration range from 5×10^{-5} to 5×10^{-3} mol dm^{-3}. Substituted *N*-arylpyrroles were:

(A) 1-(2-fluorophenyl)-2, 5-dimethylpyrrole,
(B) 1-(2-fluorophenyl)-2, 5-dimethylpyrrole -3-carbaldehyde.

The structural formulae of the investigated compounds are presented in Figures 1 and 2. The compounds were synthesized by Knorr–Paal condensation of 2,5-hexadione with the corresponding anilines [24].

The measurements were carried out in a standard electrochemical cell with a separate compartment for the reference electrode connected to the main compartment

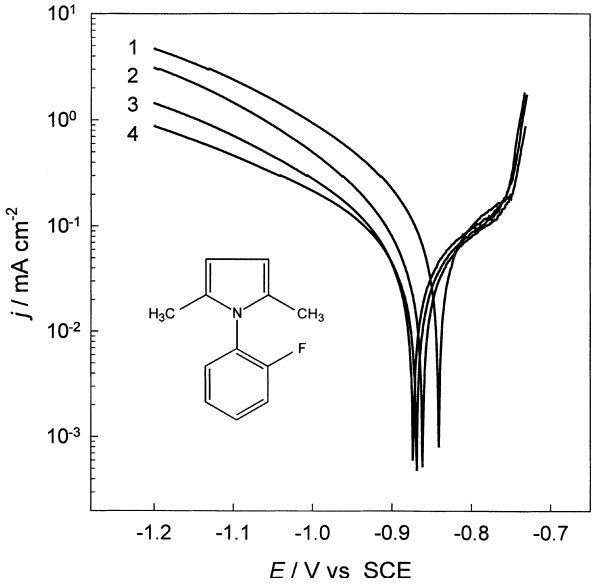

Fig. 1. Tafel plots for an aluminium electrode in 0.17 M HCl solution without (1) and in the presence of 1-(2-fluorophenyl)-2,5-dimethylpyrrole: (2) 5×10^{-4}, (3) 1×10^{-3}, (4) 5×10^{-3} M; at 20 °C, $v = 5$ mV s^{-1}.

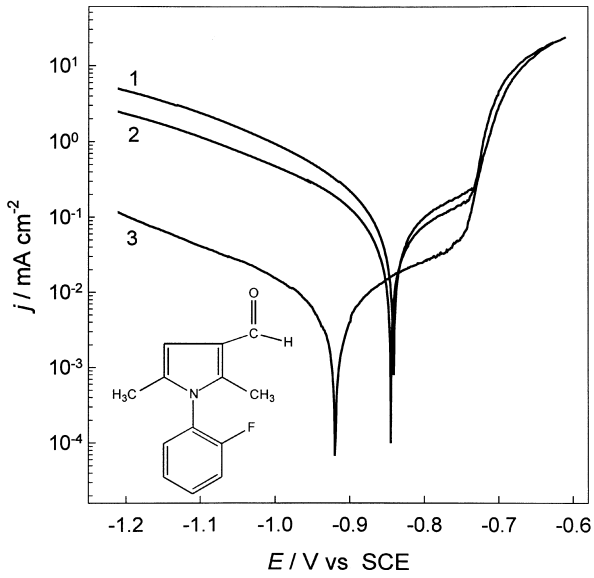

Fig. 2. Tafel plots for an aluminium electrode in 0.17 M HCl solution without (1) and in the presence of l-(2-fluorophenyl)-2,5-dimethylpyrrole-3-carbaldehyde: (2) 1×10^{-4}, (3) 5×10^{-3} M; $t = 20$ °C, $v = 5$ mV s^{-1}.

via a Luggin capillary. The cell was a water-jacket version, with a constant temperature circulator.

The polarization curves, E against j, were obtained using the linear potential sweep technique at a sweep rate of 5 mV s^{-1}, starting from the corrosion potential to the cathodic and then to the anodic side. The impedance measurements were performed in the frequency range from 60 kHz to 5 mHz with an a.c. voltage amplitude of ±5 mV. All measurements were performed using a PAR (model 273A) potentiostat and a PAR (model 5301A), lock-in amplifier, controlled by a personal computer.

3. Results and discussion

3.1. *Polarization measurements*

The potentiodynamic polarization curves for aluminium in 0.17 mol dm^{-3} HCl solution containing both inhibitors were similar in shape. Figure 1 represents the potentiodynamic polarization curves in 0.17 mol dm^{-3} HCl alone and in the presence of inhibitor A (l-(2-fluorophenyl)-2,5-dimethylpyrrole), in the concentration range from 5×10^{-5} to 5×10^{-3} mol dm^{-3}, at 20 °C. Increasing the concentration of inhibitors significantly influenced the cathodic current density, which decreased in the entire investigated potential range. The intersection points of the cathodic and anodic curves (E_{corr}) and the anodic current density were almost unaffected by the inhibitors concentration. The anodic current showed an abrupt increase at −730 mV, independent of the inhibitor concentration. It was observed that the corrosion potential shifts in the negative direction only in the presence of a higher concentration ($c > 10^{-3}$ mol dm^{-3}) of inhibitor B (1-(2-fluorophenyl)-2,5-dimethylpyrrole-3-carbaldehyde), as shown in Figure 2. This effect is probably caused by inhibitor polymerisation on the electrode surface. In this case, a passive region is observed in the potential range between E_{corr} and −730 mV where an abrupt anodic current jump occurs. It may be concluded that inhibitor B prevents localized attack on the electrode surface, as this E_{corr} shift appears to be a suitable parameter for rating resistance to localized corrosion [25].

The calculated polarization parameters, that is, E_{corr}, the cathodic Tafel slope (b_c) and the corrosion current density (j_{corr}), obtained by extrapolation of the Tafel lines, are listed in Tables 1 and 2. The large Tafel slopes ($b_c > 220$ mV div^{-1}) indicate that the hydrogen evolution reaction occurs at the metal covered by a surface layer, which acts as a potential energy barrier to the charge carriers [26, 27]. The fact that b_c values are almost equal in uninhibited and inhibited solutions suggests that the inhibitors simply block the electrode surface.

Tables 1 and 2 also list the percentages of surface coverage, θ, which is calculated using the equation:

$$\theta = \left(1 - \frac{(j_{corr})_i}{(j_{corr})_o}\right) \times 100 \qquad (1)$$

where $(j_{corr})_i$ and $(j_{corr})_o$ are the corrosion current densities in the presence and absence of inhibitor. The above equation is valid in the case when the adsorbed

Table 1. Kinetic parameters for an aluminium electrode in 0.17 mol dm^{-3} HCl solution without and in the presence of various concentrations of 1-(2-fluorophenyl)-2,5-dimethylpyrrole at 20 °C, $v = 5$ mV s^{-1}

c /mol dm^{-3}	$-b_c$ /mV	j_{corr} /mA cm^{-2}	θ /%
0	224	0.280	–
1×10^{-5}	144	0.110	60.7
5×10^{-5}	247	0.096	65.7
1×10^{-4}	242	0.089	68.2
5×10^{-4}	245	0.074	73.6
1×10^{-3}	254	0.063	77.5
5×10^{-3}	306	0.059	78.9

Table 2. Kinetic parameters for an aluminium electrode in 0.17 mol dm^{-3} HCl solution without and in the presence of various concentrations of 1-(2-fluorophenyl)-2,5-dimethylpyrrole-3-carbaldehyde at 20 °C, $v = 5$ mV s^{-1}

c /mol dm^{-3}	$-b_c$ /mV	j_{corr} /mA cm^{-2}	θ /%
0	224	0.280	–
1×10^{-5}	232	0.067	76.1
5×10^{-5}	229	0.063	77.5
1×10^{-4}	224	0.061	78.2
5×10^{-4}	227	0.027	90.4
1×10^{-3}	234	0.013	95.4
5×10^{-3}	237	0.006	97.9

molecules partially cover the electrode surface and protect the metal against corrosion. Under these conditions, the Tafel slope is the same for the supporting electrolyte as for the electrolyte containing the investigated inhibitors. The other condition that must be fulfilled in order to apply the above equation is negligible variation of the electrode potential with the inhibitor concentration [28]. The data from Tables 1 and 2 show that both conditions are completely satisfied for inhibitor A, but for inhibitor B only at the concentration less than 10^{-3} mol dm^{-3}.

3.1.1. *Effect of temperature*

The effect of temperature on the inhibiting efficiency of both inhibitors in 0.17 mol dm^{-3} HCl was determined using potentiodynamic polarization curves. The inhibitor concentration was 1.0×10^{-3} mol dm^{-3} and the temperature ranged from 20 to 60 °C. Increasing the temperature caused an increase in both the anodic and cathodic current densities, indicating that the rates of hydrogen evolution and metal dissolution, that is, the corrosion current, also increase. Since the corrosion current density increases with temperature more so in a pure HCl solution than in HCl + inhibitor, the inhibiting efficiency increases slowly with temperature. The dependence of the corrosion current on temperature can be regarded as an Arrhenius-type process, the rate of which is:

$$j_{\text{corr}} = A \exp\left(-\frac{E_a}{\mathscr{R}T}\right) \tag{2}$$

where j_{corr} is the corrosion current density, A is the Arrhenius preexponential constant, E_a is the apparent activation energy, $\mathscr{R}$ is the universal gas constant and T is the absolute temperature. Arrhenius plots (i.e., the natural logarithm of the corrosion current density against $1/T$) are presented in Figure 3. Straight lines are obtained for both pure hydrochloric acid and hydrochloric acid with added inhibitors. The calculated value of the apparent corrosion activation energy for aluminium in 0.17 mol dm^{-3} HCl is 49.6 kJ mol^{-1}, while these values are 13.4 kJ mol^{-1} in the presence of inhibitor A and 33.4 kJ mol^{-1} in the presence of inhibitor B. The decrease in $-E_a$ in the presence of inhibitors may be attributed to the chemisorption of inhibitor molecules on the metal surface. The results show a stronger chemisorption of inhibitor A than inhibitor B on the electrode surface.

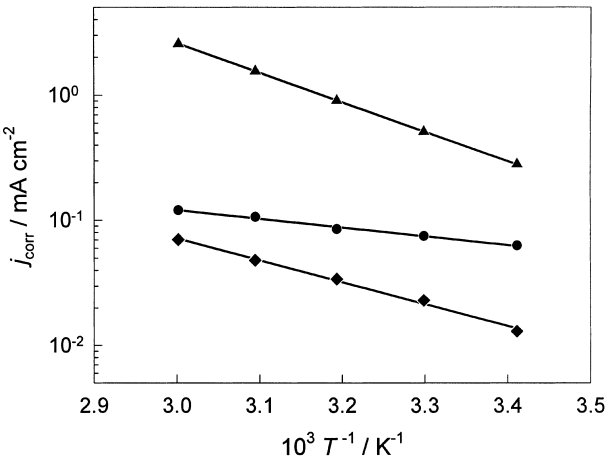

Fig. 3. Arrhenius plots of the corrosion currents obtained on the aluminium electrode in 0.17 M HCl solution without (▲) and in the presence of 1×10^{-3} M: (●) 1-(2-fluorophenyl)-2,5-dimethylpyrrole and (◆) 1-(2-fluorophenyl)-2,5-dimethylpyrrole-3-carbaldehyde.

3.1.2. *Adsorption isotherm*

To elucidate the adsorption of the studied substituted pyrroles, the type of adsorption describing the process should be determined. Basically, all available isotherms are of the form:

$$f(\theta x)\exp(-a\theta) = Kc_i \tag{3}$$

where $f(\theta x)$ is the configuration factor that depends essentially on the physical model and the assumptions underlying the derivation of the isotherm, θ is the degree of surface coverage, x is the number of water molecules replaced by the inhibitor molecule, a is the molecular interaction parameter depending on the molecular interactions in the adsorption layer and on the degree of heterogeneity of the surface, and K is the equilibrium constant of adsorption. The above equation is usually presented in the form:

$$\ln(f(\theta x)/c_i) = a\theta + \ln K \tag{4}$$

The equilibrium constant K is related to the standard free energy of adsorption, ΔG_{ads}, thus

$$K = \frac{1}{55.5}\exp\left(-\frac{\Delta G_{\text{ads}}}{\mathscr{R}T}\right) \tag{5}$$

The degree of inhibitor coverage of the metal surface is calculated using Equation 1.

Attempts were made to fit the θ values to various isotherms including the kinetic-thermodynamic models of Frumkin, Langmuir, Temkin and Flory–Huggings.

For inhibitor A, the best fit was obtained with the Frumkin and Temkin isotherms as shown in Figure 4. Applying the Frumkin isotherm:

$$Kc_i = \left(\frac{\theta}{1-\theta}\right)\exp(-2a\theta) \tag{6}$$

the values for K and a are 1.18×10^7 and -13.9, respectively, while the Temkin isotherm:

$$Kc_i = \frac{\exp(f\theta) - 1}{1 - \exp[-f(1-\theta)]} \tag{7}$$

yields the values for K and f (the factor of energetic inhomogeneity of the surface) 1.75×10^4 and 14.0, respectively.

The applicability of the Frumkin and Temkin adsorption isotherms verifies the assumption of monolayer

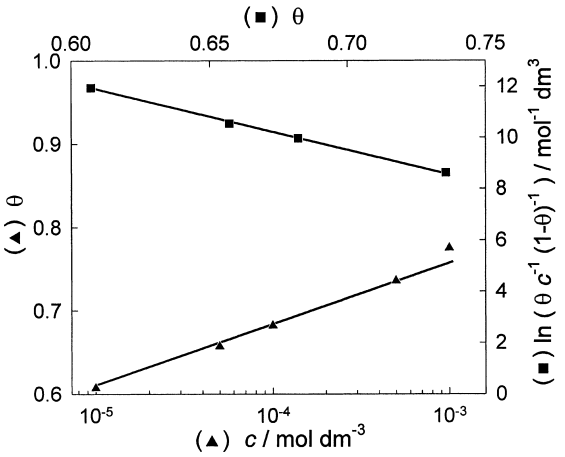

Fig. 4. Frumkin (■) and Temkin (▲) adsorption isotherms for an aluminium electrode in 0.17 M HCl solution with 1-(2-fluorophenyl)-2,5-dimethylpyrrole at 20 °C.

adsorption on an energetically uniform, inhomogeneous electrode surface with interaction in the adsorption layer. Since the effect of energetic inhomogeneity of the surface is greater than of the repulsion in the adsorption layer ($a < 0$), the Temkin isotherm is more valid [29]. The validity of the Temkin isotherm favours the assumption of a chemisorptive bond between the metal surface and the inhibitor molecules. The value of ΔG_{ads} calculated according to Equation 5 is -52.8 kJ mol^{-1}.

The acidic corrosion inhibition data for aluminium in the presence of inhibitor B can be well fitted by the Langmuir adsorption isotherm. The data give a straight line with a regression coefficient of 0.982. The equilibrium constant was determined to be 8.3×10^3, corresponding to the standard free energy of adsorption of -33.6 kJ mol^{-1}. Recently we have found [13] that acidic corrosion inhibition of aluminium in the presence of 1-(2-chlorophenyl)-2,5-dimethylpyrrole-3,4-dicarbaldehyde also follows the Langmuir adsorption isotherm.

Generally, the values of ΔG_{ads} below -20 kJ mol^{-1} are consistent with electrostatic interaction, while those above -40 kJ mol^{-1} involve chemisorption, that is, charge sharing or transfer from the inhibitor molecules to the metal surface, and coordinate type bonding [30, 31]. The values of ΔG_{ads} for both inhibitors point to the spontaneity of the adsorption process under investigated experimental conditions. The ΔG_{ads} values indicate the type of interaction between the inhibitor molecules and the metal surface. They also point out that the adsorption of investigated compounds, especially inhibitor A, occurs predominantly by chemisorption. These data correlate well with those obtained by investigation of the temperature effect on corrosion inhibition, where stronger chemisorption was observed also in the case of inhibitor A.

Investigation of the inhibitory effect of 1-phenyl-2,5-dimethylpyrroles, substituted with halogens in position 2 of the benzene ring, on corrosion of aluminium and iron in various acidic solutions [20–23] showed that substitution with the fluorine atom, due to its highest electronegativity, is the most effective. The order of inhibiting efficiency of halogens completely followed the order of Taft polar constants for ortho-substituents on a benzene ring [23]. According to the present results, further introduction of a carbaldehyde group in position 3 of the pyrrole ring causes an increase in the energy of activation and a decrease in ΔG_{ads} indicating weaker chemisorption. The higher inhibiting efficiency of this compound at higher concentration is probably caused by subsequent condensation, as pointed out earlier [20, 22].

3.2. *Electrochemical impedance spectroscopy*

Impedance measurements on the aluminium electrode in 0.17 mol dm^{-3} hydrochloric acid solution, alone and in the presence of different concentrations of inhibitors, were performed at the open-circuit potential. The obtained results are presented in the form of a Bode plot, that is, the logarithm of the impedance modulus $|Z|$ and phase angle Θ against the logarithm of a.c. frequency, f. Figures 5 and 6 represent the impedance spectra in the presence of inhibitors A and B at two particular concentrations. For comparison, the impedance spectra for aluminium in the presence of both inhibitors at a concentration of 5×10^{-3} mol dm^{-3} are presented in Figure 7. It can be seen that the curves are similar in shape. Three distinctive segments (more or less pronounced), can be observed in all cases. In the upper-frequency region, the $\log|Z|$ against $\log f$ relationship approaches zero with the phase angle values falling rapidly towards 0°. This response is typical of resistive behaviour and corresponds to solution resistance, which was about 1 Ω cm^2, in all cases. In the medium frequency region, a linear relationship between $\log|Z|$ against $\log f$ with a slope close to -1 and the phase angle approaching $-90°$, is observed. The addition of

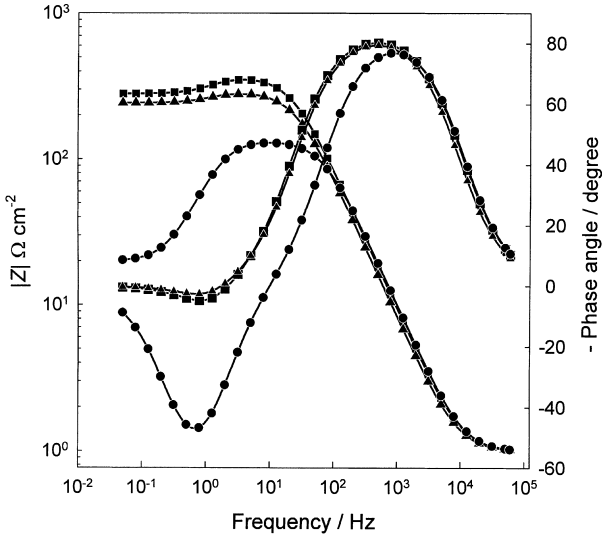

Fig. 5. Bode plots for an aluminium electrode in 0.17 M HCl solution without (●) and in the presence of (▲) 1×10^{-3} and (■) 5×10^{-3} M 1-(2-fluorophenyl)-2,5-dimethylpyrrole at 20 °C.

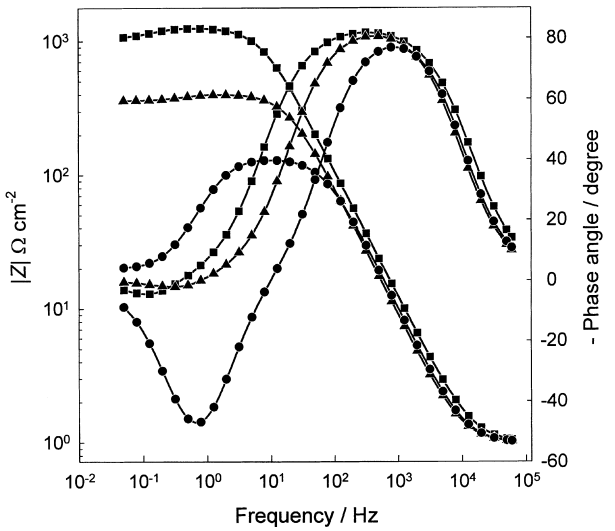

Fig. 6. Bode plots for an aluminium electrode in 0.17 M HCl solution without (●) and in the presence of (▲) 1×10^{-3} and (■) 5×10^{-3} M 1-(2-fluorophenyl)-2,5-dimethylpyrrole-3-carbaldehyde at 20 °C.

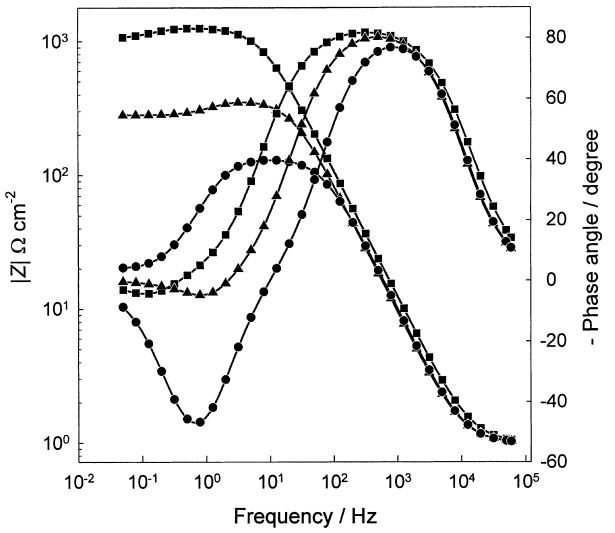

Fig. 7. Bode plots for an aluminium electrode in 0.17 M HCl solution without (●) and in the presence of 1×10^{-3} M: (▲) 1-(2-fluorophenyl)-2,5-dimethylpyrrole and (■) 1-(2-fluorophenyl)-2,5-dimethylpyrrole-3-carbaldehyde at 20 °C.

inhibitors to 0.17 mol dm^{-3} HCl does not influence the slope of the $\log|Z|$ against $\log f$ curve (the value of which was close to -0.96), it only expands the linear $\log|Z|$ against $\log f$ relationship to a lower frequency range, and causes a significant increase in the values of the impedance modulus $|Z|$. In the low frequency region, inductive behaviour is observed, which is especially pronounced for aluminium in pure hydrochloric acid solution. With increasing inhibitor concentration, the inductive behaviour of the aluminium electrode becomes less pronounced, especially in the presence of inhibitor B (Figures 6 and 7).

The impedance spectra show that at least two time constants are observed in all cases. In the investigated frequency range, similar impedance plots were reported

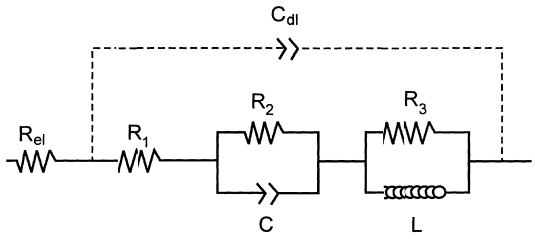

Fig. 8. Equivalent circuit diagram for the total electrode impedance.

for aluminium in various electrolytes, such as hydrochloric acid [13, 32–34], sulfuric acid [35, 36], sodium chloride [37, 38], sodium sulphate [35, 38] and acetic acid [36].

The equivalent circuit shown in Figure 8 produces an impedance plot similar to the experimental results in Figures 5–7. The transfer function of its total impedance, Z_{total} is given by

$$Z_{\text{total}} = R_{\text{el}} + \left\{ C_{\text{dl}}(\text{j}\omega) + \left[R_1 + \frac{R_2}{Z_{\text{a}}} + \frac{R_3 L^2 \omega^2}{Z_{\text{b}}} + \left(\frac{R_3^2 L}{Z_{\text{b}}} - \frac{R_2^2 C}{Z_{\text{a}}} \right)(\text{j}\omega) \right]^{-1} \right\}^{-1} \tag{8}$$

where $Z_{\text{a}} = 1 + C^2 R_2^2 \omega^2$ and $Z_{\text{b}} = R_3^2 + L^2 \omega^2$.

The procedure to extract the values of R_1, R_2, R_3, C and L consists of separating the faraday impedance by subtracting the solution resistance (1 Ω cm^2) and the double layer capacitance (20 μF cm^{-2}) [39]. The charge transfer resistance, R_{ct} is equal to the value of R_1, while the polarization resistance is equal to the sum of R_1 and R_2. The important result of this analysis is that the true transfer resistance R_{ct} is smaller than the polarization resistance R_{p}.

For each set of experimental data, the equivalent circuit parameters were evaluated using a simple least square fitting procedure. The experimental data were found to be sufficiently well fitted by the transfer function of the equivalent circuit presented in Figure 8, within the limits of experimental error and reproducibility of the data. Table 3 contains the values of impedance parameters for both inhibitors, at a concentration of 1×10^{-3} mol dm^{-3}.

Taking into account that the value of $|Z|$ is inversely proportional to the corrosion current as ω tends to zero, the values of R_1 can be used to calculate the inhibitor efficiency, $\eta_{\text{a.c.}}$:

$$\eta_{\text{a.c}} = \frac{(R_{1,\text{i}} - R_{1,\text{o}})}{R_{1,\text{i}}} \tag{9}$$

where $R_{1,\text{i}}$ and $R_{1,\text{o}}$ are resistances, with and without the presence of the inhibitor, respectively. Inhibitor efficiency increased with increasing inhibitor concentration. A higher inhibitor efficiency was observed in the presence of 1-(2-fluorophenyl)-2,5-dimethylpyrrole-3-carbaldehyde (inhibitor B), especially at higher concentrations.

Table 3. Impedance parameters for an aluminum electrode in 0.17 M hydrochloric acid solution without (0) and in the presence of inhibitors at $c = 1 \times 10^{-3}$ mol dm^{-3} and at 20 °C

Inhibitor	R_1 /Ω cm^2	R_2 /Ω cm^2	$10^6 \times C$ /F cm^{-2}	R_3 /Ω cm^2	L /H cm^2	d /nm	$\eta(R_{ct})$ /%
0	4	15	100	105	10	–	–
A	38	202	6.4	37	6	1.02	89.4
B	61	296	5.7	35	18	1.15	93.4

(A) 1-(2-fluorophenyl)-2,5-dimethylpyrrole.
(B) 1-(2-fluorophenyl)-2,5-dimethylpyrrole-3carbaldehyde
$R_1 = R_{ct}$.

Table 3 lists the inhibiting efficiency of both inhibitors, at a concentration of 1×10^{-3} mol dm^{-3}. A difference between the inhibiting efficiencies obtained using a.c. and d.c. methods does not exceed 20%, depending on the concentration of inhibitors.

Table 3 shows that the capacitance of aluminium electrode is much lower in the presence of inhibitors than in pure hydrochloric acid. The capacitance values of a few μF cm^{-2} can be attributed to the formation of a protective film on the electrode surface. Assuming a parallel plate condenser behavior, a rough estimate of the thickness values, d, for the film formed could be made by $d = \varepsilon\varepsilon_o A/C$, where ε is the dielectric constant of the surface film, ε_o is the dielectric constant of free space and A is the exposed area of the test electrode. For $\varepsilon = 7.5$ [40] and $\varepsilon_o = 8.85 \times 10^{-14}$ F cm^{-1}, the thickness values calculated for both inhibitors at a concentration of 1×10^{-3} mol dm^{-3}, and presented in Table 3, seem quite reasonable.

4. Conclusions

The corrosion behaviour of aluminium was investigated in 0.17 mol dm^{-3} hydrochloric acid with and without the addition of 1-(2-fluorophenyl)-2,5-dimethylpyrrole and its carbaldehyde derivate (position 3 in the pyrrole ring), in the temperature range 20–60 °C, using potentiodynamic and EIS techniques.

The polarization measurements showed that the inhibiting efficiency increases with increase of inhibitor concentration and solution temperature. The inhibitor decreases the values of the apparent energy of activation of the hydrogen evolution reaction. The adsorption of the *N*-arylpyrroles studied is described by the Temkin and Langmuir adsorption isotherms. The high standard free energy of adsorption, together with a decrease in the apparent energy of activation, verify the chemisorptive character of the adsorption.

All impedance spectra obtained at E_{corr} contained both high frequency capacitive and low frequency inductive parts. The electrical parameters of the proposed equivalent circuit were calculated, and the inhibiting efficiencies were determined. A satisfactory agreement in the inhibiting efficiencies obtained using a.c. and d.c. was achieved. The thickness of the protective phase layer on the electrode surface was estimated on the assumption of a parallel plate condenser behaviour.

References

1. A. Kolics, A.S. Besing, P. Baradlai, R. Haasch and A. Wieckowski, *J. Electrochem. Soc.* **148** (2001) B251.
2. M. Pourbaix, in '*Atlas of Electrochemical Equilibria in Aqueous Solutions*' (Pergamon Press, New York, 1966).
3. I. Rozenfeld 'Corrosion Inhibitors' (McGraw-Hill, New York, 1981).
4. A.A. El-Awady, B.A. Abd-El-Nabey and S.G. Aziz, *J. Electrochem. Soc.* **139** (1992) 2149.
5. D. Schweinsgberg, G. George, A. Nanayakkawa and D. Steinert, *Corros. Sci.* **28** (1988) 33.
6. G. Schmitt, *Br. Corros. J.* **19** (1984) 165.
7. T. Zhao and G. Mu, *Corros. Sci.* **41** (1999) 1937.
8. R.L. Cook, Jr and S.R. Taylor, *Corrosion* **56** (2000) 321.
9. E. Khamis and M. Atea, *Corrosion* **50** (1994) 106.
10. L. Garrigues, N. Pebere and F. Dabosi, *Electrochim. Acta* **41** (1996) 1209.
11. S.S. Mahmoud and G.A. El-Mahdy, *Corrosion* **53** (1997) 437.
12. A.S. Fouda, M.N. Moussa, F.I. Taha and A.I. El Neanea, *Corros. Sci.* **26** (1986) 719.
13. M. Metikoš-Huković, R. Babić and Z. Grubač, *J. Appl. Electrochem.* **28** (1998) 433.
14. R. Babić, M. Metikoš-Huković, S. Omanović, Z. Grubač and S. Brinić, *Br. Corros. J.* **30** (1995) 288.
15. M. Metikoš-Huković, R. Babić, Z. Grubač and S. Brinić, *J. Appl. Electrochem.* **24** (1994) 325.
16. M. Metikoš-Huković, R. Babić, Z. Grubač and S. Brinić, *J. Appl. Electrochem.* **24** (1994) 772.
17. E. Khamis, B.A. Abd El-Nabey, M. Shaban, A. El-Sharnoby and G.E. Thomson, *in* Proceedings of the 7th European Symposium on 'Corrosion Inhibitors', Ann. Univ. Ferrara, N.S., Sez. V, Suppl. N. 9 (1990), p. 1173.
18. M.S. Abdel-Aal, M. Th. Makhlof and A.A. Hermas, *in* Proceedings *op. cit.* [17], p. 1143.
19. G. Trabanelli, *in* F. Mansfeld (Ed.), 'Corrosion Inhibitors', (Marcel Dekker, New York, 1987), chapter 3.
20. M. Metikoš-Huković, Z. Grubač and E. Stupnišek-Lisac, *Corrosion* **50** (1994) 146.
21. M. Metikoš-Huković, R. Babić and Z. Grubač, *J. Appl. Electrochem.* 32 (2002) 35.
22. E. Stupnišek-Lisac and M. Metikoš-Huković, *Br. Corros. J.* **28** (1993) 74.
23. E. Stupnišek-Lisac, M. Metikoš-Huković, D. Lenčić, J. Vorkapić-Furač and K. Berkovič, *Corrosion* **48** (1992) 924.
24. J. Vorkapić-Furač, M. Mintas, T. Burgemeister and A. Mannschreck, *J. Chem. Soc. Perkin Trans.* **2** (1989) 713.
25. C. Monticelli, G. Brunoro and G. Trabanelli, *in* Proceedings, *op. cit.* [17], p. 1125.
26. A.K. Vijh, *J. Phys. Chem.* **73** (1969) 506.

27. R.E. Mayer, *J. Electrochem. Soc.* **113** (1966) 1158.
28. Z. Szklarska-Smialowska and M. Kaminski, *Corros. Sci.* **11** (1971) 843.
29. A.E. Stoyanova, E.I. Sokolova and S.N. Raicheva, *Corros. Sci.* **39** (1997) 1595.
30. S.K. Rangarajan, *J. Electroanal. Chem.* **82** (1977) 93.
31. J.O'M. Bockris and D.A.J. Swinkels, *J. Electrochem. Soc.* **111** (1964) 736.
32. E.J. Lee and S.I. Pyun, *Corros. Sci.* **37** (1995) 157.
33. C.M.A. Brett, *Corros. Sci.* **33** (1992) 203.
34. C.M.A. Brett, *J. Appl. Electrochem.* **20** (1990) 1000.
35. J.H. de Wit and H.J.W. Lenderink, *Electrochim. Acta* **41** (1996) 1111.
36. J.W. Lenderink, M. Linden and J.H. de Wit, *Electrochim. Acta* **38** (1993) 1989.
37. S.E. Frers, M.M. Stefenel, C. Mayer and T. Chierchie, *J. Appl. Electrochem.* **20** (1990) 996.
38. J.B. Bessone, D.R. Salinas, C. Mayer, M. Ebert and W.J. Lorenz, *Electrochim. Acta* **37** (1992) 2283.
39. W.J. Lorenz and F. Mansfeld, *Corros. Sci.* **21** (1981) 647.
40. R.C. Weast, 'Handbook of Chemistry and Physics' (Chemical Rubber Co., Cleveland, 1990), pp. 6–144.